Selective Catalytic Reduction of NO with Hydrocarbons: Experimental and Simulation Results

Gesthimani D. Lionta, Sophia C. Christoforou, Evangelos A. Efthimiadis,*,† and Iacovos A. Vasalos

Chemical Process Engineering Research Institute and Department of Chemical Engineering, Aristotelian University of Thessaloniki, P.O. Box 1517, 54006 University City, Thessaloniki, Greece

The selective catalytic reduction (SCR) of NO was studied over alumina-based catalysts. The experimental data showed that the peak NO conversion and the temperature range where each catalyst exhibits its highest activity depend on the impregnated metal. Kinetic studies were carried out to estimate the apparent order of reaction with respect to the involved gases and the apparent activation energies. The catalytic activity of the alumina-based catalysts was also tested in a fixed-bed reactor unit under various reaction conditions. A mathematical model was applied to reproduce the experimental data using the experimentally determined reaction rate expression. The model predictions were in agreement with the concentrations measured at the exit of the fixed-bed reactor, though no arbitrarily chosen parameters were used in the application of the mathematical model.

Introduction

Nitrogen oxides (NO_x) are gaseous pollutants that contribute to the acid rain formation, the photochemical air pollution, and the depletion of the ozone layer. Other problems linked with the presence of nitrogen oxides in the atmosphere are health problems to humans, like bronchitis, pneumonia, and susceptibility to viral infections. The main sources of NO_x emissions in the atmosphere from human activities are power plants, boilers, and vehicles' engines. Catalytic processes have been developed to convert the NO_x to nitrogen and thus limit the environmental pollution. Recently, research is focused on the replacement of ammonia from deNOx units of power plants with hydrocarbons. The ammonia slip, the corrosion of equipment, and the storage of ammonia are operational problems that are solved by replacing ammonia with hydrocarbons, which probably already exist in the inlet gas stream of deNOx units. The catalytic reduction of NO_x with hydrocarbons is described by the following reaction:

$$2a\mathrm{NO}_x + b\mathrm{HC} + c\mathrm{O}_2 \xrightarrow{\text{cat.}} a\mathrm{N}_2 + d\mathrm{CO}_2 + e\mathrm{H}_2\mathrm{O} \quad (1)$$

where HC is the hydrocarbon and a, b, c, d, and e are the appropriate stoichiometric coefficients.

Tabata et al. (1994) studied the patent literature of selective catalytic reduction (SCR) catalysts. They classified these catalysts in two basic categories: catalysts based on zeolites (usually ZSM-5 and Mordenite) and catalysts based on metal oxides (mainly alumina). Their survey showed that though a large number of catalysts has been developed and tested, none was selected for commercial application, because the catalytic performance of each catalyst depends strongly on the involved reaction conditions. The SCR of NO on metal-exchanged zeolites was examined by Burch and Scire (1994). The order of the catalytic activity changed with the presence or absence of oxygen and with the use of ethane or methane as reductant in the reactive gas. An outline of the development of SCR catalysts is described by Iwamoto and Yahiro (1994). Hamada (1994) examined the catalytic activity of catalysts based on metal oxides. Experimental results showed that factors that affect the activity of this group of catalysts are the solid acidity or basicity and the presence of transition metals of high oxidation activity on the metal-supported oxides.

Methane is among the nonselective hydrocarbons, according to the classification of Iwamoto and Hamada (1991), that can be used as the reductant for the catalytic reduction of NO. Experimental studies showed that zeolite-based catalysts exhibit catalytic activity for the NO reduction with methane in the presence of oxygen (Ga/ and Co/ZSM5 in the work of Li and Armor (1994) and Ga/ and In/ZSM5 in the work of Kikuchi and Yogo (1994)). However, when alumina (Hamada, 1994) or alumina-based (Li and Armor, 1994) catalysts were tested for the same reaction, low activities were measured. The catalytic performance of alumina is significantly improved when higher hydrocarbons (selective reductants) take the place of methane. Propene is selectively consumed in the NO reduction rather than in the propene oxidation. Mechanistic studies were carried out to develop a reaction scheme for copper-exchanged zeolites (Burch and Millington, 1993) and for Pt/alumina catalysts (Burch et al., 1994) when propene is the reductant.

The aim of previous research works on the SCR of NO was the experimental testing of catalysts under various reaction conditions and the elucidation of the reaction mechanism that dominates during the selective NO reduction. In this study, we examined the effect of the impregnated metal on the activity of the catalyst and we performed kinetic studies to develop a reaction rate expression that describes the NO reduction rate over a Pt/alumina catalyst. This catalyst was used in fixed-bed experiments, as well. The scope of this work was, therefore, to combine the kinetic, the fixed-bed, and the modeling studies as follows: The reaction rate expression was employed in the application of the mathematical model, and the mathematical model results were validated with experimental data measured in the fixed-bed reactor. In this way we combined experimental results measured under differential and integral conditions with predictions of a mathematical model that does not use fitting parameters.

* Author to whom correspondence should be addressed.
† E-mail address: EFTHIMIA@CLIO.CPERI.FORTH.GR.

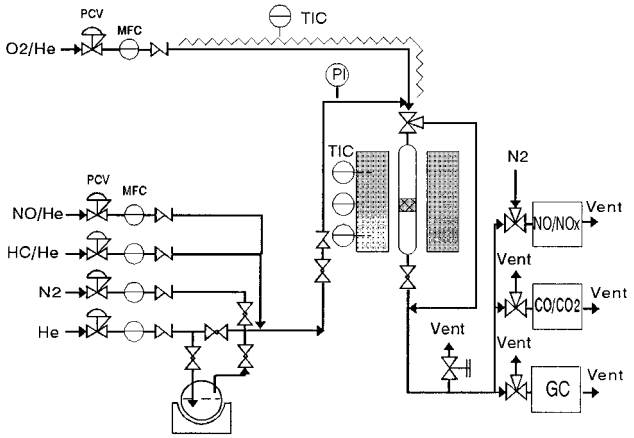

Figure 1. Schematic of the catalytic reaction unit.

Materials

Metal/alumina catalysts were prepared using the impregnation technique. γ-Alumina extrudates were supplied by Engelhard. The extrudates were crushed and sieved to separate the particles of 180−355 μm. Pt/alumina was prepared by the impregnation of alumina with hexachloroplatinic acid solution. Co/, Ni/, and Cu/alumina were prepared using nitrate solutions of the corresponding metals. All catalysts contained about 2 % wt of the impregnated metal. Following the impregnation, the catalysts were dried at 120 °C and then calcined at 500 (Co, Cu, and Pt) or 600 °C (Ni). A reforming catalyst with the commercial name CK303 was also supplied from Ketjen-Akzo. The content of this catalyst in Pt was 0.3 wt %, and it was in the extrudates form. This catalyst was precalcined at 500 °C in air for 2 h before the SCR experiments.

The composition of each catalyst was determined by the inductively coupled plasma and atomic emission spectroscopy (ICP/AES) technique. The pore size distribution of the catalysts was measured using the mercury porosimetry technique. The overall pore volume was 0.5 cm^3/g, and the pore diameters varied in the range of 0.005−0.02 μm, mainly. The BET surface area of the catalysts was in the range of 165−176 m^2/g. Nitrogen adsorption measurements showed that the surface areas of the fresh and the reacted catalyst were the same. The physicochemical properties and the catalytic activity of catalysts prepared in different batches were, within experimental error, the same.

Experimental Setup and Procedure

Reactivity experiments were carried out in the catalytic reaction unit shown in Figure 1. The unit consists of the feed gas system, a three-zone furnace controlled by PID controllers, and the gas analysis system. The catalytic reduction of NO took place in a quartz flow reactor of 2 cm o.d. The catalyst was placed in the middle of two 1 cm long zones of inert material (silica). A K-type thermocouple was located in the middle of the catalytic bed and another thermocouple of the same type was located at the exit of the catalytic bed. The difference between the indication of the two thermocouples was used to estimate the temperature change due to the chemical reaction. NO reduction experiments were carried out at different reaction temperatures in the range of 150−600 °C.

Mass flow controllers were used to control the flow rate of gases of standard composition (2% NO in He, 2% C_3H_6 in He, 20% O_2 in He, and pure He). We preheated the inlet gas stream at 150 °C to prevent the NO oxidation (Zhang and Flytzani-Stephanopoulos, 1994). The composition of the reactive gas during the NO_x reduction experiments was 500−3500 ppmv NO, 1000−3500 ppmv C_3H_6, and 5% O_2 in He. The flow rate of the inlet gas was 1000 mL/min, and the reactor loading was 4 or 0.5 g. As a result, the catalyst to flow ratio (W/F) was 0.24 or 0.03 g s cm^{-3}, respectively.

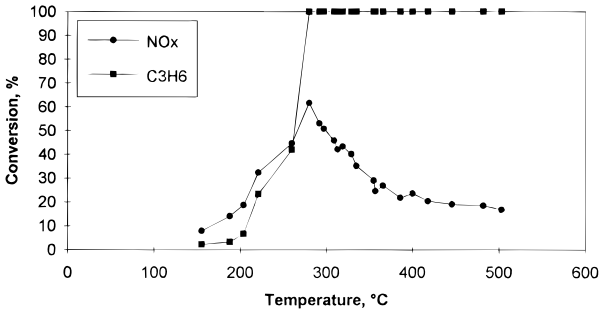

Figure 2. Effect of the reaction temperature on the NO_x and C_3H_6 conversion over Pt/alumina: NO, 2000 ppmv; C_3H_6, 2000 ppmv; O_2, 5%; total flow rate, 1000 mL/min; catalyst weight, 4 g.

Samples from the exit gas stream were analyzed to determine the extent of the SCR reaction and to identify the gas products. The nitrogen oxides (NO and NO_2) were measured in a NO_x analyzer of Thermo Environmental, Model 42H. The concentrations of CO and CO_2 were measured in a Dual Channel NDIR analyzer of Rosemount, Model NGA 2000. Gas samples were automatically injected in a Varian 3600 CX gas cromatograph, equipped with TCD and FID detectors. A molecular sieve 13X column was used for the separation of the inorganic species and a Haysep N column for the separation of the organic species. Gas mixtures of standard composition were used to calibrate the gas analysis system.

Experimental results were collected when the concentrations of the reactive gases at the exit of the reactor and the reaction temperature remained unchanged (steady state). The NO_x conversion, defined as the percentage of the inlet NO that is converted to N_2 and N_2O, is used in the presentation of our experimental data. When the effect of the NO or the C_3H_6 concentration on the reaction rate was studied, the concentration of the other involved gases and the reaction temperature were constant.

Results and Discussion

Fixed-Bed Experiments. Initially we examined the thermal reduction of NO in an empty reactor (blank experiments) under our reaction conditions. No thermal nitric oxide reduction was measured in the temperature range of 150−500 °C. The selective reduction of NO was studied over different metal/alumina catalysts experimentally under the following reaction conditions: The reactor was loaded with 4 g of catalyst, the flow rate was 1000 mL/min (W/F = 0.24 g s cm^{-3}), and the reactive gas mixture was 2000 ppmv NO, 2000 ppmv C_3H_6, and 5% O_2 in He.

The reactivity data over the Pt/alumina catalyst are shown in Figure 2. The NO_x and the propene conversions are presented as a function of the reaction temperature. The analysis of the product gas stream showed that the reacted propene is almost completely converted to CO_2 (and extremely low concentrations of CO), while NO was converted to N_2, NO_2, and N_2O. The selectivity of the NO reduction toward N_2O was low, as

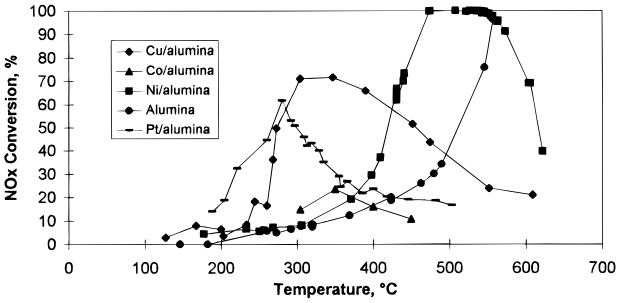

Figure 3. Comparison between the NO_x vs temperature curves over metal/alumina catalysts: NO, 2000 ppmv; C_3H_6, 2000 ppmv; O_2, 5%; total flow rate, 1000 mL/min; catalyst weight, 4 g.

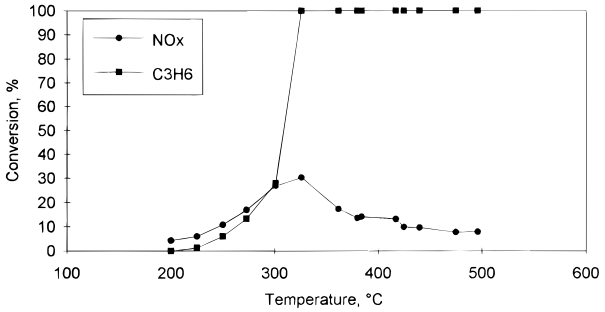

Figure 4. Effect of the reaction temperature on the NO_x and C_3H_6 conversion over the CK303 Pt/alumina catalyst: NO, 1000 ppmv; C_3H_6, 1000 ppmv; O_2, 5%; total flow rate, 1000 mL/min; catalyst weight, 2 g.

it will be discussed later in this section. As a result, in the presentation of our experimental data we display the NO_x conversion. The evolution of the NO_x conversion with the reaction temperature exhibits a typical volcano-type curve. Comparison between the NO_x and C_3H_6 conversion curves of Figure 2 shows that the peak NO_x conversion is measured at the temperature where propene is consumed completely. This implies that the NO reduction proceeds competitively with the oxidation of propene.

The NO_x conversion vs temperature curves for the alumina support and the alumina-based catalysts are displayed in Figure 3. The experiments in this figure were carried out under the reaction conditions used in the previous figure. The dependence of the propene conversion on the reaction temperature was similar to that shown in Figure 2.

We tested the possibility that the alumina support reduces the NO. The experimental data in Figure 3 show low but steadily increasing reactivity with temperature. At high temperatures (>500 °C) complete conversion of both NO_x and C_3H_6 was measured. The catalytic activity of alumina for the SCR reaction was also examined by Miyadera (1993) and by Hamada et al. (1991) under reaction conditions different from those of this study. Our results and those of the above two works imply that alumina cannot effectively reduce the NO and that active sites should be incorporated in the porous support to improve its reduction ability. A possible interpretation for this behavior is given by the reaction mechanism of Burch et al. (1994), where the initial step for the SCR of NO is the reduction of the surface oxygen by propene. The impregnation of active sites on the support solid decreases the temperature where this reduction takes place.

The catalytic activity of Co/alumina (Figure 3) was low and almost constant in the temperature range of 300−450 °C. Hamada et al. (1991) also noticed that Co/alumina prepared from cobalt nitrate is inactive for the SCR of NO. However, the same authors measured a significant increase in the activity of Co/alumina prepared from cobalt acetate. The results of X-ray photoelectron spectra studies suggested that when Co/alumina is prepared from a nitrate solution, the main species in the catalyst is Co_3O_4. On the other hand, when the catalyst is prepared from an acetate solution, Co forms cobalt aluminates. It was, thus, postulated that the latter compounds are active for the SCR of the NO. Consequently, the preparation procedure of the catalyst can be a significant parameter that can change its catalytic activity.

The experimental data over Ni/alumina show that NO is completely reduced at relatively high temperatures

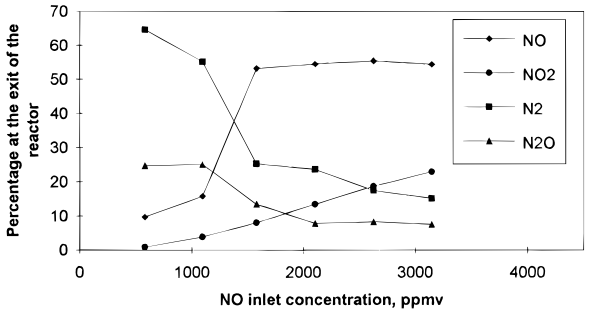

Figure 5. Distribution of nitrogen-containing gases at the exit of the reactor for different initial NO concentrations: reaction temperature, 228 °C; C_3H_6, 2000 ppmv; O_2, 5%; total flow rate, 1000 mL/min; catalyst weight, 4 g.

(475−550 °C), while those over Cu/alumina show that the maximum NO_x conversion is about 70% (temperature range: 300−400 °C) (Figure 3). The light-off temperature over the Pt/alumina catalyst is 275 °C, and the NO_x conversion at this temperature is 62%. The comparison between the experimental data over different alumina-based catalysts indicates that the impregnation of Pt, Ni, and Cu on the support enhances significantly the NO reduction and that the peak NO_x conversion and the temperature range where each catalyst exhibits its peak activity depend on the impregnated metal.

The catalytic performance of the commercial Pt/alumina CK303 catalyst is shown in Figure 4. The reactive gas mixture was 1000 ppmv NO, 1000 ppmv C_3H_6, and 5% O_2 in He, the inlet gas flow rate was 1000 mL/min, and the reactor loading was 2 g. The NO_x conversion dependence on the reaction temperature over the CK303 catalyst exhibited its peak activity at somehow higher temperatures than those of the Pt/alumina catalyst prepared in our laboratory, and lower NO_x conversions were measured with respect to those in Figure 2, for a given reaction temperature. These differences can be attributed to the Pt content (0.3 and 2 % wt in the CK303 and the laboratory prepared catalysts, respectively) and to the variation in the reaction conditions.

The effect of the NO concentration on the gas products of the SCR reaction is presented in Figure 5. The reaction temperature in the experiments of this figure was 228 °C, and the reaction conditions were identical to those used in Figures 2 and 3. The selectivity to NO_2, N_2, and N_2O was defined as the percentage of the inlet NO that was converted to these gases. The formation of nitrogen and dinitrogen monoxide can be explained by the reaction mechanism of Burch et al. (1994). This

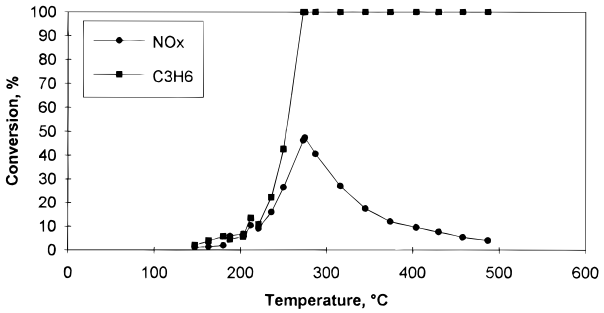

Figure 6. Effect of the reaction temperature on the NO_x and C_3H_6 conversion over Pt/alumina: NO, 1000 ppmv; C_3H_6, 1000 ppmv; O_2, 5%; total flow rate, 1000 mL/min; catalyst weight, 0.5 g.

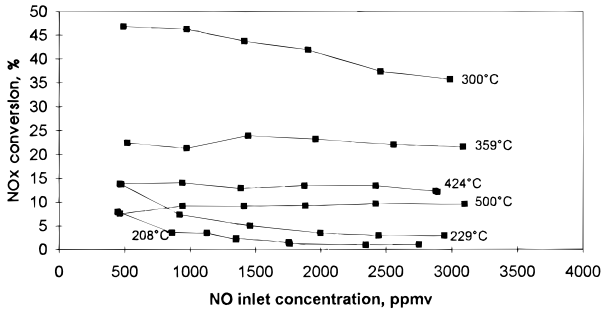

Figure 7. Effect of the NO concentration on the NO_x conversion at different temperatures: reaction temperature, 228 °C; C_3H_6, 1000 ppmv; O_2, 5%; total flow rate, 1000 mL/min; catalyst weight, 0.5 g.

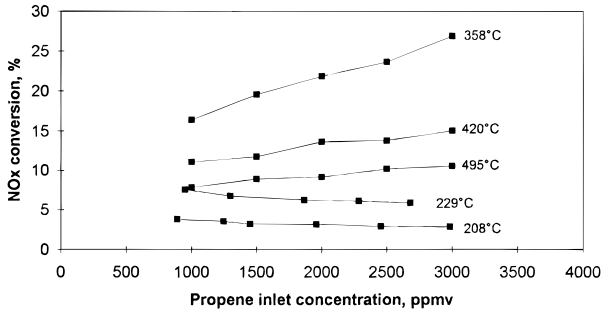

Figure 8. Effect of the C_3H_6 concentration on the NO_x conversion at different temperatures: reaction temperature, 228 °C; NO, 1000 ppmv; O_2, 5%; total flow rate, 1000 mL/min; catalyst weight, 0.5 g.

mechanism involves the reduction of surface Pt atoms and, subsequently, the NO reduction over the reduced sites. Nitrogen is formed from the recombination of adjacent nitrogen atoms, and N_2O, from the reaction of nitrogen atoms with adsorbed NO molecules. According to the above mechanism the production of N_2O is low at temperatures higher than the light-off temperature (275 °C for the Pt/alumina of this study). The experimental data in Figure 5 show that an increase in the initial NO concentration enhances the formation of NO_2 and increases the concentration of the unreacted NO at the exit of the reactor. As a result, the NO_x conversion decreased with an increase in the NO inlet concentration. The selectivity to N_2 was high at low NO inlet concentrations, while it dropped significantly at higher NO concentrations. The selectivity to N_2O followed the same trend with that to nitrogen, though the concentration of N_2O was relatively low.

Kinetic Studies. Noble metal-based catalysts are expected to be more stable than transition metal-based catalysts. This is the reason that we chose to perform our kinetic studies with the Pt/alumina catalyst, though higher activities were measured for the Cu/ and Ni/alumina catalysts. Experimental data over the Pt/alumina catalyst are presented in Figure 6 in the temperature range of 150−500 °C. Low reactive gas concentrations (1000 ppmv NO, 1000 ppmv C_3H_6, and 5% O_2 in He) and reactor loading (0.5 g) were used in this series of experiments. As a result, the conversion of the reactive gases was relatively low and we considered that the reactor operates differentially. The experimental data in Figure 6 follow the same trend as those in Figure 2 with the NO conversions in the former figure lower than those in the latter figure. The experimental data presented in Figure 6 were compared to those of Burch et al. (1994) (a 2% Pt in alumina catalyst prepared from hexachloroplatinic acid) because in both studies the same preparation procedure and similar reaction conditions (catalyst to flow ratio: 0.03 g s cm^{-3} and low NO and propene concentrations) were applied. This comparison showed a good agreement between the experimental data of the two studies, though experiments were carried out in reactors of different dimensions (2 and 0.7 cm o.d.).

Reaction rates in the temperature range of 150−250 °C were plotted as a function of the inverse absolute temperature to estimate the apparent activation energies for the NO_x and the C_3H_6. The NO_x and the C_3H_6 consumption rates gave apparent activation energies of 13.7 ± 2.2 and 11.3 ± 2.8 kcal/mol, respectively. These values are in a good agreement with those reported by Jen and Gandhi (1994) (15 ± 3 and 13 ± 2 kcal/mol, respectively) for the SCR of NO with C_3H_6 over a Cu/alumina catalyst ($W/F = 0.02$ g s cm^{-3}). Higher activation energies were estimated by Gopalakrishnan et al. (1993) (20 kcal/mol) and by Zhang et al. (1994) (26 kcal/mol) from the reduction rates of NO over Cu/ZSM5 and La_2O_3, respectively.

We varied the NO and the C_3H_6 concentrations and we correlated the NO_x reduction rates with the reactive gas concentrations to estimate the apparent orders of reaction with respect to the involved gases. Experimental data for different NO and C_3H_6 concentrations are shown in Figures 7 and 8, respectively. These experiments were carried out under the following reaction conditions: the reactor was loaded with 0.5 g of the Pt/alumina catalyst, the feed gas flow rate was 1000 mL/min, and its composition was 5% O_2, 500−3000 ppmv NO, 1000−3000 ppmv C_3H_6, and He as balance. When we examined the effect of the NO (or C_3H_6) concentration on the reduction rate, the C_3H_6 (or NO) concentration was 1000 ppmv.

The NO_x conversion in Figure 7 increases with the temperature in the range of 208−300 °C and decreases with the temperature in the range of 300−500 °C for a given NO concentration. This behavior is consistent with the volcano-type curve of Figure 6. At relatively low temperatures (208−300 °C) the NO_x conversion decreases as the NO concentration in the inlet gas stream increases. It is, therefore, expected that at these temperatures the apparent order of reaction is fractional. The analysis of the experimental data at 229 °C gave an apparent order of reaction with respect to NO of 0.375. The fractional order of reaction implies that at these temperatures the reaction proceeds via adsorbed species. On the other hand, at higher temperatures (359−500 °C) the NO_x conversion does not change with the NO concentration. The analysis of these kinetic data (i.e., the variation of the reaction rate

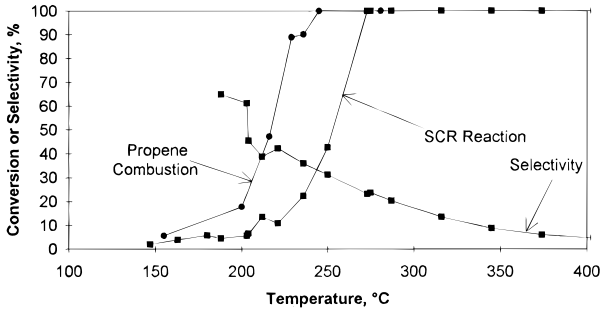

Figure 9. Propene consumption during the SCR of NO and the oxidation of propene: NO, 1000 ppmv; C_3H_6, 1000 ppmv; O_2, 5%; total flow rate, 1000 mL/min; catalyst weight, 0.5 g.

with the NO concentration) gave an apparent order of reaction with respect to the NO concentration of about 1.

The variation of the NO conversion with the propene content in the feed gas is shown in Figure 8. An increase in the propene concentration gives rise to higher NO_x conversion at 358, 420, and 495 °C, while at lower temperatures (208 and 229 °C) the NO_x conversion changes slightly with the hydrocarbon concentration. The analysis of the kinetic data at 358, 420, and 495 °C for different propene concentrations gave an apparent order of reaction with respect to propene in the range of 0.25−0.55. A similar temperature dependent order of reaction with respect to the propene concentration was noticed by Jen and Gandhi (1994).

The propene conversion vs temperature curves in Figures 2 and 6 are almost identical, though these experimental data were measured under different reaction conditions. In Figure 9 we present the propene oxidation in the absence of NO in the feed gas (the NO was replaced by He) along with the propene consumption during the SCR of NO. Comparison between these two curves shows a shift of the propene conversion curve toward higher temperatures when NO is present in the feed gas. This implies that NO reduction and propene oxidation takes place on the same active sites. In the same figure we present the selectivity of the propene consumption for the SCR reaction. We define the selectivity for the SCR reaction as the percentage of propene that is consumed during this reaction. Propene is effectively used for the NO reduction at low temperatures, while at higher temperatures the oxidation of propene dominates.

Development of a Mathematical Model

The mathematical models used in the simulation of chemical reactors where the NO reduction takes place can be roughly classified in two categories: those models that develop an analytical expression for the NO concentration along the reactor and those models that use numerical techniques to solve the problem. In the former case a first order reaction rate dependence with respect to the reactive gas gives rise to mathematical expressions that can be solved analytically. This approach was used by Buzanowski and Yang (1990) to simulate the catalytic reduction of NO with NH_3. In the latter case a complex reaction rate expression is used (for instance, a rideal-type rate expression (Tronconi et al., 1992), and numerical approximations are used to simulate the performance of the reactor.

We considered a pseudohomogeneous model in the development of our mathematical model of a fixed-bed reactor. The problem was solved for isothermal and nonisothermal operation of the reactor. The mass and energy balances for the reactive gases are

$$D_b \frac{\partial^2 C_i}{\partial z^2} - u \frac{\partial^2 C_i}{\partial z} - R = 0 \qquad (2)$$

$$\lambda \frac{\partial^2 T}{\partial z^2} - \rho u c_p \frac{\partial T}{\partial z} + (-\Delta H)R - 4\frac{U_H}{d_r}(T - T_r) = 0 \qquad (3)$$

where i is the reactive gas species, C_i is the concentration of the gas species, D_b is the axial dispersion coefficient, u is the axial velocity, z is the axial distance, L is the reactor length, R is the reaction rate, ρ is the gas density, c_p is the heat capacity, d_r is the reactor diameter, T is the temperature in the reactor, T_r is the temperature of surroundings, λ is the effective thermal conductivity, $(-\Delta H)$ is the heat of reaction, and U_H is the overall heat transfer coefficient.

Standard boundary conditions were used for the solution of eqs 2 and 3.

Boundary Conditions.

$$u(C_{oi} - C_i) = -D_b \frac{\partial C_i}{\partial z} \qquad \text{at } z = 0 \qquad (4)$$

$$\rho u c_p (T_o - T) = -\lambda \frac{\partial T}{\partial z} \qquad \text{at } z = 0 \qquad (5)$$

$$\frac{\partial C_i}{\partial z} = \frac{\partial T}{\partial z} = 0 \qquad \text{at } z = L \qquad (6)$$

When isothermal operation of the reactor was considered, eq 3 and the corresponding boundary conditions were not employed.

Numerical Procedure

A program developed in CPERI based on the finite element method was used to solve the system of the nonlinear partial differential equation. The physical domain was divided into N subdomains ($N = 8$ in this study), and within each interval the solution was approximated by a function $f(x,y) = \sum_{i=1}^{N} a_i \phi^i(x,y)$, where a_i are coefficients to be found and ϕ^i are known finite element basis functions. We used linear basis functions defined on the standard domain $0 < \xi < 1$. The Galerkin's method of weighted residuals reduced the N differential equations to a system of nonlinear algebraic equations: $\tilde{J}\tilde{U} = -\tilde{R}$, where $\tilde{J}$ is the Jacobean of the system, $\tilde{U}$ is the vector of the unknown variables, and $\tilde{R}$ is the matrix of the residuals. The Newton iteration and the LU decomposition method were employed to solve the algebraic system.

Model Validation

The validation of the mathematical model was carried out using the experimental data over the Pt/alumina catalyst of this study and those of Li and Armor (1993) over Co/ZSM5 and Mn/ZSM5. In the application of the mathematical model we employed kinetic data determined from independent experiments performed under differential reaction conditions, while the other involved reaction parameters were either calculated or measured. The model predictions were compared with experimental data measured in fixed-bed reactors.

The temperature difference between the gas phase and the catalyst surface was negligible according to the

Table 1. Reaction Conditions and Kinetic Data Used in the Application of the Mathematical Model

	for given catalyst		
	Pt/alumina	Co/ZSM-5	Mn/ZSM-5
initial reaction temp, °C	228	400	400
space velocity at the initial reaction temp, h^{-1}	7500	7500	7500
Pecklet no. at the initial reaction temp	14.4	167.6	167.6
reactor i.d., cm	1.7	0.5	0.5
bed height, cm	3.5	4	4
apparent activation energy, cal/g-mol	13 740	10 500	10 500
NO concentration, ppmv	1000−2500	350−1800	350−1800
HC concentration, ppmv	2000	250−2050	250−2050
catalyst weight, g	4	0.4	0.4
bed voidage	0.4	0.4	0.4
order w.r.t. NO concentration	0.375	0.44	0.52
order w.r.t. CH_4 concentration	0	0.56	0.59
reaction rate const at the initial reaction temp, $\rho_b k_o$	3×10^{-5} (g-mol/cm^3)$^{0.625}$/s	11 586 1/s	63 753 (cm^3/g-mol)$^{0.11}$/s

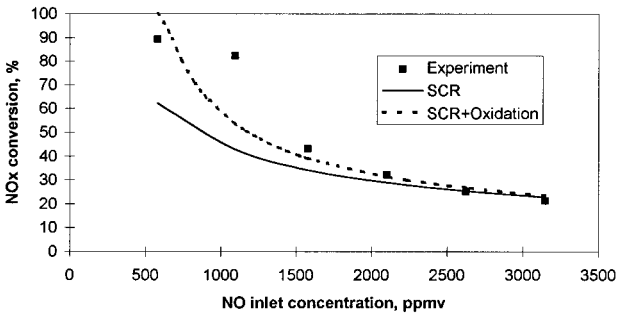

Figure 10. Experimental data over Pt/alumina and model predictions: C_3H_6, 2000 ppmv; O_2, 5%; total flow rate, 1000 mL/min; catalyst weight, 4 g.

criteria of Mears (1971). An effectiveness factor of unity was estimated using the generalized Thiele modulus (Froment and Bischoff, 1979), implying the absence of intraparticle diffusional limitations.

The variation of the NO conversion with the NO concentration in Figure 7 at 229 °C gave an apparent order of reaction of 0.375 with respect to the NO concentration, while the NO reduction rate remained almost constant when the propene concentration changed (Figure 8). As a result, we considered that the NO reduction rate is described by the following expression: $R = \rho_b k[C_{NO}]^{0.375}$, where ρ_b is the apparent density of the catalyst (0.5 g/cm^3) and k is the reaction rate constant. The apparent activation energy was also estimated experimentally as it was described in the kinetic studies of this work. The effective diffusivity in the catalyst bed (D_b) was estimated from the bulk diffusion coefficient of NO in a He stream, assuming that the tortuosity factor in the bed is 2 and that the porosity in the bed is 0.4. We used standard correlations (Bird et al., 1960; Perry and Chilton, 1973) to calculate the values of the other reaction parameters (heat capacity, thermal conductivity, heat of reaction, and heat transfer coefficient). A parametric investigation was carried out to study the sensitivity of our predictions to the effective diffusivity. Our results showed insignificant changes in the predicted conversions when D_b was changed by 1 order of magnitude. The application of our mathematical model does not require the use of any arbitrarily chosen parameter since the involved parameters are either calculated or estimated experimentally. The kinetic data and the reaction conditions that were used in the application of the mathematical model are listed in Table 1.

Experimental results over the Pt/alumina catalyst are presented in Figure 10 along with mathematical modeling predictions (continuous line, labeled SCR) for different NO inlet concentrations. The variation of the NO conversion with the NO concentration in this figure follows the same trend as that of Figure 7 at 229 °C, but the NO conversion in the former figure is significantly higher than that of the latter figure for a given NO concentration. Model predictions were calculated for isothermal operation of the reactor because our experimental measurements were collected when the gas concentrations at the exit of the reactor and the reaction temperature were constant.

Our mathematical model can adequately reproduce the experimental data for NO concentrations higher than 2000 ppmv, while at lower concentrations the experimentally measured NO conversion was higher than the predicted NO conversion. No propene was detected at the exit gas stream when the NO concentrations was low (500-1000 ppmv). Complete consumption of the propene was also noticed at higher reaction temperatures (above the peak temperature), where the apparent order of reaction was unity (Figure 2). In the above mathematical model we did not account for the oxidation of propene. This reaction is highly exothermic, leading to higher temperatures on the catalyst surface. However, a temperature rise enhances the NO and the propene conversions as shown in Figure 2. In conclusion, we attribute the difference between the experimental results and the model predictions in Figure 10 to the oxidation of propene that was not consumed in the SCR reaction. This reaction leads to a local temperature rise along the reactor that cannot be predicted by this mathematical model. Kinetic data for the propene oxidation—when NO is present—are needed to include the oxidation reaction in our mathematical model.

When we extended the above mathematical model to account for the two reactions that take place in the catalytic bed (NO reduction and C_3H_6 oxidation), we needed a reaction rate expression for the oxidation of propene that would predict the inhibition caused by the presence of NO in the feed gas stream according to the experimental evidence. Therefore, we considered that the propene oxidation rate is proportional to the propene concentration and inversely proportional to the NO concentration leading to the following expression: $R_{ox} = \rho_b k_{ox} \exp(-E_{ox}/RT)[C_{HC}]/[C_{NO}]$, where R_{ox} is the propene oxidation rate, ρ_b is the apparent catalyst density, k_{ox} is the frequency factor, E_{ox} is the apparent activation energy, T is the reaction temperature, $[C_{HC}]$ is the propene concentration, and $[C_{NO}]$ is the NO concentration. The dependence of the propene oxidation rate on the NO concentration was attributed to our belief that NO reduction and propene oxidation take place on the same active sites and that at temperatures lower than the peak temperature the former reaction

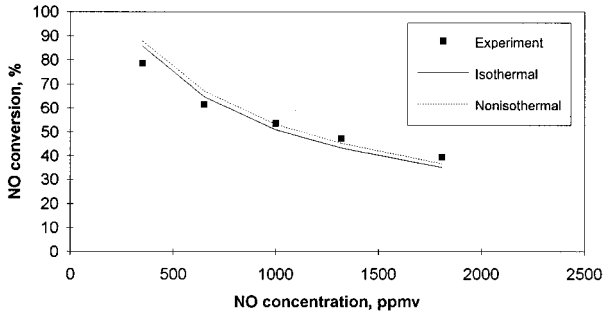

Figure 11. Experimental data over Co/ZSM5 (Li and Armor, 1993) and model predictions. CH_4, 820 ppmv; O_2, 2.5%; total flow rate, 100 mL/min; catalyst weight, 0.4 g.

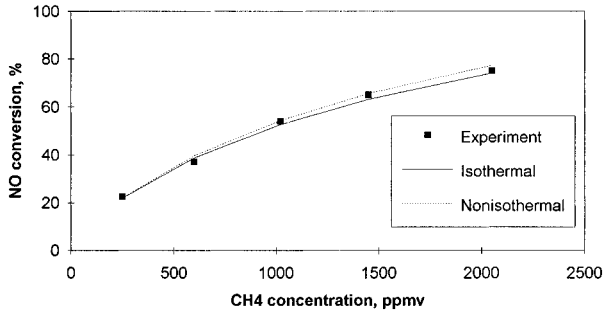

Figure 12. Experimental data over Mn/ZSM5 (Li and Armor, 1993) and model predictions. NO, 820 ppmv; O_2, 2.5%; total flow rate, 100 mL/min; catalyst weight, 0.4 g.

dominates. The apparent activation energy (E_{ox} = 15 250 cal/mol) was estimated from the correlation of the propene oxidation rate with the temperature and the frequency factor ($\rho_b k_{ox}$ = 0.5 gmol/cm^3/s) was calculated from the propene oxidation rate in experiments where the NO concentration was in the range of 2000−3000 ppmv in the feed gas stream. In these experiments the propene conversion was lower than 30%. In the application of the extended model we employed the reaction conditions and the kinetic data of Table 1 and the above reaction rate expression for the oxidation of propene. Nonisothermal operation of the reactor was considered in these simulation studies.

The simulation results for the extended model are shown in Figure 10 (dashed line, labeled SCR+Oxidation). The experimental data are in better agreement with the extended model predictions (SCR+Oxidation) than with simplified model predictions (SCR). We attribute this difference to the predicted temperature rise along the axis of the reactor as a result of the propene oxidation.

Li and Armor (1993) performed differential experiments (reactor loading of 0.05 g and gas consumption of less than 20%) to calculate the reaction rate dependence on the NO the CH_4 concentrations. We estimated the reaction rate constant at the reaction temperature from the reaction rates measured by Li and Armor when the reactor was loaded with 0.05 g of catalysts Co/ZSM-5 and Mn/ZSM-5. In the same study SCR experiments were also carried out over the above catalysts using a larger catalyst weight (0.4 g).

The experimental data of Li and Armor (1993) are compared with our model predictions in Figures 11 and 12. The experimental data are presented along with the mathematical model predictions for isothermal and nonisothermal operation of the reactor. In the latter case a small temperature rise in the reactor, of the order of 2−3 °C, was predicted. The CH_4 concentration in Figure 11 is 820 ppmv, the NO concentration varied in the range of 250−2050 ppmv, the reactor loading was 0.4 g of catalyst Co/ZSM5, and the reaction temperature was 400 °C. A similar comparison is presented in Figure 12 for the Mn/ZSM5 catalyst, a constant NO concentration (820 ppmv), and different CH_4 concentrations (350−1800 ppmv) at 400 °C. Good agreement is noticed between the experimental and the modeling data for both catalysts. The above experimental data and model predictions show that high methane and low nitric oxide concentrations lead to higher NO conversions. Model results were also compared with experimental data over the Co/ZSM5 catalyst for different methane concentrations (constant NO concentration) and over the Mn/ZSM5 catalyst for different NO concentrations (constant CH_4 concentration). The agreement between our predictions and the experimental data was similar to that shown in Figures 11 and 12.

Conclusions

Experimental data over alumina-based catalysts showed that the impregnated metal affects the extent of the SCR reaction, the shape of the NO conversion vs temperature curve, and the temperature range where the peak NO conversion is measured. The Ni/alumina catalyst exhibited the highest activity between the catalysts tested in this work, but at relatively high temperatures. The Cu/alumina catalyst reduced up to 70% of the NO at lower temperatures. Relatively low activation energies (13.7 kcal/mol for the NO and 11.3 kcal/mol for the C_3H_6) were estimated from the Arrhenius plot of the NO reduction rate for both NO and C_3H_6 over Pt/alumina. Kinetic studies showed that the apparent order of reaction with respect to the NO concentration is unity in the temperature range of 359−500 °C and fractional at lower temperatures. The NO reduction rate did not change significantly with the propene concentration at temperatures lower than the light-off.

Numerical techniques were employed to simulate the performance of a fixed-bed reactor. The model results were validated with the experimental data of this study and with those of Li and Armor (1993). The agreement between the experimental data and the simulation data was efficient, though in the application of the mathematical models we did not use arbitrarily chosen parameters.

Acknowledgment

This work was funded by the Commission of the European Community, under Contract EV5V-CT094-0535.

Literature Cited

Bird, R. B.; Stewart, W. E.; Lightfoot, E. N. *Transport Phenomena*; Wiley: New York, 1960.
Burch, R.; Millington, P. J. *Appl. Catal. B* **1993**, *2*, 101.
Burch, R.; Scire, S. *Appl. Catal. B* **1994**, *3*, 295.
Burch, R.; Millington, P. J.; Walker, A. P. *Appl. Catal. B* **1994,** *4*, 65.
Buzanowski, M. A.; Yang, R. T. *Ind. Eng. Chem. Res.* **1990**, *29*, 2074.
Froment, G. F.; Bischoff, K. B. *Chemical Reactor Analysis and Design*; Wiley: New York, 1979.
Gopalakrishnan, R.; Stafford, P. R.; Davidson, J. E.; Hecker, W. C.; Bartholomew, C. H. *Appl. Catal. B* **1993**, *2*, 165.
Hamada, H. *Catal. Today* **1994**, *22*, 21.
Hamada, H.; Kintaichi, Y.; Sasaki M.; Ito, T. *Appl. Catal.* **1991,** *75*, L1.

Iwamoto, M.; Hamada, H. *Catal. Today* **1991,** *10*, 57.
Iwamoto, M.; Yahiro, H. *Catal. Today* **1994**, *22*, 5.
Jen, H. W.; Gandhi, H. S. *Environmental Catalysis*; ACS Symposium Series 552; American Chemical Society: Washington, DC, 1994; p 53.
Kikuchi, E.; Yogo, K. *Catal. Today* **1994,** *22*, 73.
Li, Y.; Armor, J. N. *Appl. Catal. B* **1993**, *2*, 239.
Li, Y.; Armor, J. N. *J. Catal.* **1994,** *145*, 1.
Mears, D. E. *J. Catal.* **1971**, *20*, 127.
Miyadera, T. *Appl. Catal. B* **1993,** *2*, 199.
Perry, R. H.; Chilton, C. H. *Chemical Engineers' Handbook*; McGraw-Hill: Tokyo, 1973.
Tabata, T.; Kokitsu, M.; Okada, O. *Catal. Today* **1994**, *22*, 147.
Tronconi, E.; Forzatti, P.; Martin J. P. G.; Malloggi, S. *Chem. Eng. Sci.* **1992,** *47*, 2401.
Zhang, Y.; Flytzani-Stephanopoulos, M. *Environmental Catalysis*; ACS Symposium Series 552; American Chemical Society: Washington, DC, 1994; p 7.
Zhang, X.; Walters, A. B.; Vannice, M. A. *Appl. Catal. B* **1994**, *4*, 237.

Received for review December 11, 1995
Accepted May 7, 1996[⊗]

IE950752F

[⊗] Abstract published in *Advance ACS Abstracts,* July 15, 1996.